

Local structure studies of Ti for SrTi¹⁶O₃ and SrTi¹⁸O₃ by advanced X-ray absorption spectroscopy data analysis

A Anspoks¹, J Timoshenko¹, D Bocharov¹, J Purans¹, F Rocca², A Sarakovskis¹, V Trepakov^{3,4}, A Dejneka⁴ and M Itoh⁵

¹ Institute of Solid State Physics, University of Latvia, Riga, LV-1063, Latvia

² IFN-CNR, Institute for Photonics and Nanotechnologies, Unit 'FBK-Photonics' of Trento, Povo (Trento), Italy

³ Ioffe Physical-Technical Institute RAS, St-Petersburg, Russia

⁴ Institute of Physics, AS CR, Prague, Czech Republic

⁵ Tokyo Institute of Technology, Japan

andris.anspoks@cfi.lu.lv

Strontium titanate is a model quantum paraelectric in which, in the region of dominating quantum statistics, the ferroelectric instability is inhibited due to nearly complete compensation of the harmonic contribution into ferroelectric soft mode frequency by the zero-point motion contribution. The enhancement of atomic masses by the substitution of ¹⁶O with ¹⁸O decreases the zero-point atomic motion and low-T ferroelectricity in SrTi¹⁸O₃ is realized. In this study we report on the local structure of Ti in SrTi¹⁶O₃ and SrTi¹⁸O₃ by Ti K-edge extended x-ray absorption fine structure measurements in temperature range 6 - 300 K.

Introduction

Strontium titanate (SrTiO₃, STO) is a well-known and thoroughly studied model that is representative of the family of ABO₃ oxides and related materials [1]. At room temperature it has the cubic O_h¹ perovskite-type structure. Upon cooling, STO undergoes a second order *Pm3m* (O_h¹) to *I4/mcm* (D_{4h}¹⁸) antiferrodistorsive (AFD) phase transition (PT) at $T_C = 105$ K, with condensation of the R_{25} phonon mode at the Brillouin zone boundary [2, 3]. Following the Barrett formula [4, 5], the dielectric permittivity at first rises strongly upon cooling due to softening of the lowest TO₁ phonon mode (incipient ferroelectricity). At low temperatures, where the quantum statistics dominates the rising of dielectric permittivity saturates and the ferroelectric ordering is suppressed by quantum effects. The paraelectric phase of STO is retained down to the lowest temperatures (quantum paraelectricity [5, 6, 7]). This leads to the idea that ferroelectricity in STO can be induced by suppression of the quantum fluctuations. Experimentally, this was observed using isotope exchange (¹⁶O with ¹⁸O) [8].

There is long debate about the structure of the polar phase and the mechanism of the phase transition in $\text{SrTi}^{18}\text{O}_3$. The first mechanism proposed was the displacive type, caused by the condensation of the ferroelectric E_u soft mode [9, 10, 11, 12], the second was the addition of an order-disorder type component to the displacive soft mode one [13, 14, 15, 16].

The structure of STO has been studied by different experiments: X-ray diffraction (XRD) [17, 18], neutron diffraction [19, 20] and X-ray absorption spectroscopy [21, 22, 23, 24, 25, 26, 27, 28] but clear picture and consistence of opinions have not yet been achieved.

In this work the local atomic structure around Ti in $\text{SrTi}^{16}\text{O}_3$ and $\text{SrTi}^{18}\text{O}_3$ is studied in the temperature range 8 - 300 K with X-ray absorption spectroscopy methods, namely extended x-ray absorption fine structure (EXAFS), advanced reverse Monte Carlo (RMC) and evolutionary algorithm (EA) techniques for EXAFS data analysis (RMC/EA-EXAFS) [29].

Experimental

In our study we used two powder samples: standard $\text{SrTi}^{16}\text{O}_3$ (STO16) with 100% ^{16}O (STO16) and $\text{SrTi}^{18}\text{O}_3$ (STO18) where 96 % of ^{16}O atoms were substituted by ^{18}O isotope. STO18 sample crystals preparation procedure has been previously described in ref.[9].

The Ti K-edge x-ray absorption spectra were measured in transmission mode at the ESRF bending-magnet beamline BM23 and at the HASYLAB/DESY A1 bending-magnet beamline in the temperature range 6 K - 300 K. The x-ray radiation was monochromatized by a Si(111) double-crystal monochromator, and the beam intensity was measured using two ionization chambers filled with argon and krypton gases. The temperature of the sample was stabilized on ± 0.1 K with He flow cryostat. To achieve the best sample homogeneity and thickness at the Ti K-edge, necessary for transmission mode experiments, the proper amount of the STO powder was deposited on polytetraflouroethylene Millipore membranes from suspensions in methyl alcohol.

The EXAFS oscillations signals $\chi(k)$ were extracted following the conventional procedure [30, 31] using the EDA software package [32].

The extracted STO16 EXAFS spectra $\chi(k)k^2$ and corresponding Fourier transforms are shown in Fig. 1. Spectra of STO18 and STO16 look very similar, as it was expected since difference in the structure between STO18 and STO16 is very small [8]. The peak of the first coordination shell (seen in Fourier transform between 1 and 2 Å) contains only the single scattering signal. The peaks located between 2.5 and 4 Å correspond to the second (Sr atoms) and the third (Ti atoms) coordination shells of Ti, which are very close and cannot be independently analysed; moreover they contain multiple scattering contributions from different Ti-O-Ti chains and triangles. At the same time, one can see that Ti-Sr contribution is very sensitive towards temperature, unlike the ones from Ti-Ti and Ti-O.

RMC/EA-EXAFS simulations

The best method to analyze these data is to use reverse Monte Carlo (RMC) and evolutionary algorithm (EA) techniques for EXAFS data analysis (RMC/EA-EXAFS) [29]. The method does not restrict the geometry of the system (in our case no limitations to the distortions of the oxygen octahedra and positions of Ti and Sr atoms in it) and takes into account all multiple scattering effects, which are very sensitive to the bonding angles and distances, e.g. in Ti-O-Ti chains and triangles.

In RMC/EA-EXAFS simulations we used 32 supercells, where each supercell with size $4a \times 4b \times 4c$ contains 1280 atoms. Lattice constants a , b and c were taken from diffraction studies [20]. Comparison of the experimental and theoretical EXAFS spectra has been performed using a Morlet wavelet transform (WT) [33, 34] in $3 \text{ \AA}^{-1} - 16 \text{ \AA}^{-1}$ of the k -space, and $0.9 \text{ \AA} - 4.5 \text{ \AA}$ of the R -space range.

Being a straightforward mathematical procedure as the Fourier transform, the WT allows one to obtain a two-dimensional representation of the periodic signal with simultaneous localization in k and R spaces that is an advantage over conventional fit in k or R space only. In the case of STO, for instance, WT allows one to discriminate the contributions from Ti-Ti and Ti-Sr atom pairs. Also differences between STO18 and STO16 spectra can be better noticed using the WT method than the standard EXAFS analysis methods.

The use of WT for data fitting in our case has also the advantage that it allows to better separate the contribution to the total EXAFS of the first coordination shell (Ti-O) from the noise due to imperfections in background subtraction procedure.

Scattering paths with the half-path length up to 5.5 \AA and the multiple-scattering contributions up to the third order were considered in our simulations. The calculation of the cluster potential was performed only once for the average atom configuration, corresponding to the SrTiO_3 crystallographic structure. The complex exchange-correlation Hedin-Lundqvist potential and default values of muffin-tin radii, as provided within the FEFF8 code [35], were employed. As the output of RMC/EA-EXAFS analysis we have obtained a set of atomic coordinates, which can be used to calculate radial distribution functions, average distance between atoms, MSRD, and other values.

Results and discussion

The obtained radial distribution functions (RDF) for Ti-O in the first coordination shell are shown in Fig.3, where two distinct groups of the oxygen atoms separated by about 0.1 \AA are evident for STO18 in the whole range of temperatures. At the same time, the RDFs for STO16 contain less pronounced features, however the broad non-Gaussian shape of the Ti-O RDF remains in the whole range of temperature.

Evidences of similar distortions were previously documented for STO by Fisher et.al. [21] and for BaTiO₃ by Ravel et.al. [36,37]. On the contrary, the presence of a single dominating distance between Ti-Ti is shown in Fig.4: this is a sign of strong correlation between neighboring Ti atoms.

The RDF corresponding to the distribution of Ti-Sr distances shows strong temperature dependence (Fig.5). The shape of the RDF does not change significantly; all features only flatten with the increase of the temperature, indicating increasing thermal disorder.

The mean-square relative displacement (MSRD) values are shown in Fig. 6 and 7. MSRDs are calculated as the second moment of the RDF. At the first glimpse, one can see that all values do not follow classical Einstein-like temperature behaviour, especially for STO18.

It is seen that the absolute values of Ti-O MSRD in the low temperature region for STO18 are larger than those for STO16. This confirms our previous studies using X-ray absorption near edge structure studies [38]. This is mainly due to the presence of the displacements of Ti atoms from the central position, as already documented by Ti-O RDF (Fig.3). This effect is much bigger than that we can expect by applying an Einstein model only on the grounds of isotopic substitution [39].

The values of Ti-O MSRD for STO18 show a quite well distinguishable peak around 25 K, where transition to polar phase occurs. This can be a sign of fluctuations, leading to larger dynamic and/or static displacements of Ti in the oxygen octahedra.

The Ti-Ti MSRD temperature dependence for STO18 and STO16 (Fig.6) is nearly flat till 110K. Above the AFD PT point, it slightly increases and again remains nearly constant at least in the temperature range 150 – 250 K.

The values of Ti-Sr MSRD show an Einstein-like temperature behaviour in the high temperature region (in cubic phase). For STO18, a jump-like discontinuity at 25 K is shown by the values of Ti-Sr MSRD. These increased values at polar phase may be correlated with the observed increased static disorder for Ti. No anomalies are observed for Ti-Sr MSRD for STO16 in the low temperature region.

Conclusions

The obtained results show a clear non-Gaussian character of the RDFs for the first three coordination shells of Ti, especially for the first shell in the studied whole temperature range (6 – 300 K).

We have found that there are well resolved two groups of oxygen atoms (separated by $\sim 0.1\text{\AA}$) in the first coordination shell of Ti in STO18, in the whole range of the temperatures. The same applies to STO16, but the corresponding distance between two groups of oxygen atoms is smaller.

The absolute values for the first coordination shell of Ti (Ti-O) MSD in the low temperature region for STO18 are larger than those for STO16. The MSD values for the first coordination shell of Ti in STO18 have noticeable anomaly in the vicinity of the low-T phase transition into polar phase (25 K).

At the same time, there is a strong correlation between nearest neighbouring Ti atoms for STO18 in the whole range of the temperatures. Ti-Ti MSD values show noticeable anomaly around AFD PT in the 105 - 150 K region.

MSD for Ti-Sr have the strongest temperature dependence, with Einstein-like temperature behaviour in the high temperature region, corresponding to the cubic phase. Ti-Sr MSD for STO18 shows jump-like discontinuity at 25 K which may be correlated with the observed increased static disorder for Ti. No anomalies are observed for Ti-Sr MSD for STO16 in the low temperature region.

The nature of these effects observed can be static or dynamic. It is important that our measurements revealed the presence of some static and dynamic disorders in STO16, more pronounced in STO18. It can be connected to precursor effect widely discussed today [40]. It was suggested that a strongly frustrated state in STO at low temperatures is realized due to an interaction between the structural and ferroelectric order parameters. Such low temperature state of STO was treated as a critical one near the paraelectric-ferroelectric phase transition. In such scenario, pronunciation of polar ordering precursor effects in STO-18 in comparison with STO-16 looks quite natural.

Acknowledgements

This work has been supported by the Latvian Science Council grant no. 402/2012. The work was supported in part from the large infrastructure SAFMAT Project CZ.2.13/3.1.00/22132, P108/12/1941 of GACR and PP RAS “Quantum mesoscopic and disordered systems”. The authors thank Dr. Olivier Mathon from ESRF and Dr. Edmund Welter from DESY for assistance during the measurements, and Dr. Alexei Kuzmin for fruitful discussions and feedback.

References

- [1] Lines M E and Glass A M 1977 Principles and Applications of Ferroelectrics and Related Materials (Oxford: Clarendon Press) p 680
- [2] Fleury P A, Scott J F, and Worlock J M: SOFT PHONON MODES AND THE 110°K PHASE TRANSITION IN SrTiO₃. Phys. Rev. Lett. 1968;21: 16-19
- [3] Shirane G, and Yamada Y: Lattice-Dynamical Study of the 110 K Phase Transition in SrTiO₃. Phys. Rev. 1969; 177: 858-863
- [4] Barrett J H: Dielectric Constant in Perovskite Type Crystals. Phys. Rev. 1952 ;86: 118-120.
- [5] Muller K A and Burkard H: SrTiO₃: An intrinsic quantum paraelectric below 4 K. Phys. Rev. B 1979;19: 3593-3602

- [6] Vaks V G 1973 Introduction to Microscopical Theory of Ferroelectrics (Moscow: Nauka) p 327 (in Russian)
- [7] Kvyatkovskii O E : Quantum Effects in Incipient and Low-Temperature Ferroelectrics (A Review). Phys. Sol. State 2001;43 1345-1362.
- [8] Itoh M, Wang R, Inaguma Y, Yamaguchi T, Shan Y J, and Nakamura T: Ferroelectricity Induced by Oxygen Isotope Exchange in Strontium Titanate Perovskite. Phys. Rev. Lett. 1999;82: 3540-3543
- [9] Taniguchi H, Itoh M, and Yagi T: Ideal Soft Mode-Type Quantum Phase Transition and Phase Coexistence at Quantum Critical Point in ^{18}O -Exchanged SrTiO_3 . Phys. Rev. Lett. 2007;99: 017602
- [10] Hasebe H, Tsujimi Y, Wang R, Itoh M, and Yagi T: Dynamical mechanism of the ferroelectric phase transition of SrTiO_3 studied by light scattering. Phys. Rev. B 2003;68: 014109
- [11] Takesada M, Itoh M, and Yagi T: Perfect Softening of the Ferroelectric Mode in the Isotope-Exchanged Strontium Titanate. Phys. Rev. Lett. 2006;96: 227602
- [12] Deng H-Y, Lam C-H, Huang H T: On the origin of oxygen isotope exchange induced ferroelectricity in strontium titanate. Eur. Phys. J. B 2012;85: 234
- [13] Blinc R, Zalar B, Laguta V V, Itoh M: Order-Disorder Component in the Phase Transition Mechanism of ^{18}O Enriched Strontium Titanate. Phys. Rev. Lett. 2005;94: 147601
- [14] Shigenari T, Abe K, Takemoto T, Sanaka O, Akaike T, Sakai Y, Wang R, and Itoh M: Raman spectra of the ferroelectric phase of $\text{SrTi}^{18}\text{O}_3$: Symmetry and domains below T_c and the origin of the phase transition. Phys. Rev. B 2006;74: 174121
- [16] Scott J F, Bryson J, Carpenter M A, Herrero-Albillos J, and Itoh M: Elastic and Anelastic Properties of Ferroelectric $\text{SrTi}^{18}\text{O}_3$ in the kHz-MHz Regime. Phys. Rev. Lett. 2011;106: 105502.
- [15] Bussmann-Holder A and Bishop A R: Incomplete ferroelectricity in $\text{SrTi}^{18}\text{O}_3$. Eur. Phys. J. B 2006;53: 279-282.
- [17] Lytle F W: XRay Diffractometry of Low Temperature Phase Transformations in Strontium Titanate. J. Appl. Phys. 1964;35: 2212-2215.
- [19] Heidemann A and Wettengel H: Die Messung der Gitterparameter/änderung von SrTiO_3 . Z. Phys. 1973;258: 429-438.
- [20] Hui Q, Tucker M G, Dove M T, Wells S A, Keen D A: Total scattering and reverse Monte Carlo study of the 105 K displacive phase transition in strontium titanate. J. Phys.: Condens. Matter 2005;17: S111-S124
- [Dawber2005] Dawber M, Rabe K M, and Scott J F: Physics of thin-film ferroelectric oxides. Rev. Mod. Phys. 2005;77: 1083-1130.
- [18] Schmidbauer M, Kwasniewski A and Schwarzkopf J: High-precision absolute lattice parameter determination of SrTiO_3 , DyScO_3 and NdGaO_3 single crystals. Acta Cryst. B 2012;68: 8-14.
- [21] Fischer M, Lahmar A, Maglione M, San Miguel A, Itie J P, and Polian A: Local disorder studied in SrTiO_3 at low temperature by EXAFS spectroscopy. Phys. Rev. B 1994;49: 12451-12456.

- [22] Ravel B and Stern E A: Local disorder and near edge structure in titanate perovskites. *Physica B* 1995;208/209: 316-318.
- [23] Kamishima O, Nishihata Y, Maeda H, Ishii T, Sawada A, and Terauchi H: EXAFS study on the local structure in strontium titanate. *Physica B* 1995;208/209: 303-304
- [24] Nozawa S, Iwazumi T, and Osawa H: Direct observation of the quantum fluctuation controlled by ultraviolet irradiation in SrTiO₃. *Phys. Rev. B* 2005;72: 121101
- [25] Andreasson B P, Janousch M, Staub U, Meijer G I, Delley B: Resistive switching in Cr-doped SrTiO₃: An X-ray absorption spectroscopy study. *Mat. Sci. Eng. B* 2007;144: 60-63
- [26] Hashimoto T, Yoshiasa A, Okube M, Okudera H and Nakatsuka A: Temperature dependence of XANES spectra for ATiO₃, A₂TiO₄ and TiO₂ compounds with structural phase transitions. *AIP Conf. Proc.* 2007;882: 428-430.
- [27] Vračar M, Kuzmin A, Merkle R, Purans J, Kotomin E A, Maier J, and Mathon O: Jahn-Teller distortion around Fe⁴⁺ in Sr(Fe_xTi_{1-x})O_{3-δ} from x-ray absorption spectroscopy, x-ray diffraction, and vibrational spectroscopy. *Phys. Rev. B* 2007;76: 174107
- [28] Levin I, Krayzman V, Woicik J C, Tkach A, and Vilarinho P M: X-ray absorption fine structure studies of Mn coordination in doped perovskite SrTiO₃. *Appl. Phys. Lett.* 2010;96: 052904
- [30] Rehr J J and Albers R C: Theoretical approaches to x-ray absorption fine structure. *Rev. Mod. Phys.* 2000; 72: 621-654.
- [31] Aksenov VL, Kovalchuk MV, Kuzmin A, Purans J, Tyutyunnikov SI: Development of methods of EXAFS spectroscopy on synchrotron radiation beams, *Crystallogr. Rep.* 2006; 51: 908-935.
- [29] Timoshenko J, Kuzmin A, Purans J: EXAFS study of hydrogen intercalation into ReO₃ using the evolutionary algorithm. *J. Phys.: Condens. Matter* 2014;26: 055401.
- [33] Munoz M, Argoul P, Farges F : Continuous Cauchy wavelet transform analyses of EXAFS spectra: a qualitative approach. *Am. Mineral.* 2003;88: 694-700.
- [34] Timoshenko J, Kuzmin A: Wavelet data analysis of EXAFS spectra. *Comp. Phys. Commun.* 2009;180: 920-925.
- [32] Kuzmin A: EDA: EXAFS data analysis software package. *Physica B* 1995;208-209: 175-176
- [35] Ankudinov AL, Ravel B, Rehr JJ and Conradson SD: Real-space multiple-scattering calculation and interpretation of x-ray-absorption near-edge structure. *Phys. Rev. B* 1998;58: 7565 - 7576.
- [36] Ravel B, Stern E A, Vedralinskii R I, and Kraizman V: Local Structure and the Phase Transition of BaTiO₃. *Ferroelectric* 1998;206: 407-430
- [37] Stern EA: Character of Order-Disorder and Displacive Components in Barium Titanate. *Phys. Rev. Lett.* 2004;93: 037601.
- [38] A. Anspoks, D. Bocharov, J. Purans, F. Rocca, A. Sarakovskis, V. Trepakov, A. Dejneka, M. Itoh: Local structure studies of SrTi₁₆O₃ and SrTi₁₈O₃. *Phys. Scripta* 2014;89: 044002

[39] Purans J., Afify N.D., Dalba G., Grisenti R., De Panfilis S., Kuzmin A., Ozhogin V. I., Rocca F., Sanson A., Tiutiunnikov S. I. and Fornasini P.: Isotopic Effect in extended x-ray-absorption fine structure of Germanium. Phys. Rev. Letters 2008;100:055901.

[40] Bussmann-Holder A., Beige H and G. Völkel G: Precursor effects, broken local symmetry, and coexistence of order-disorder and displacive dynamics in perovskite ferroelectrics. Phys. Rev B 2009;79: 184111.

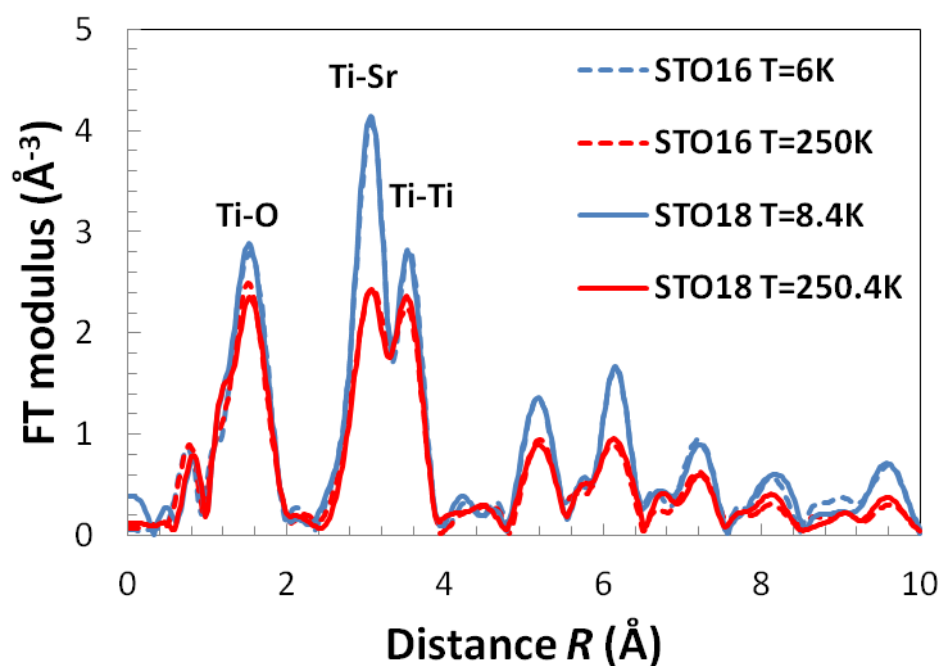
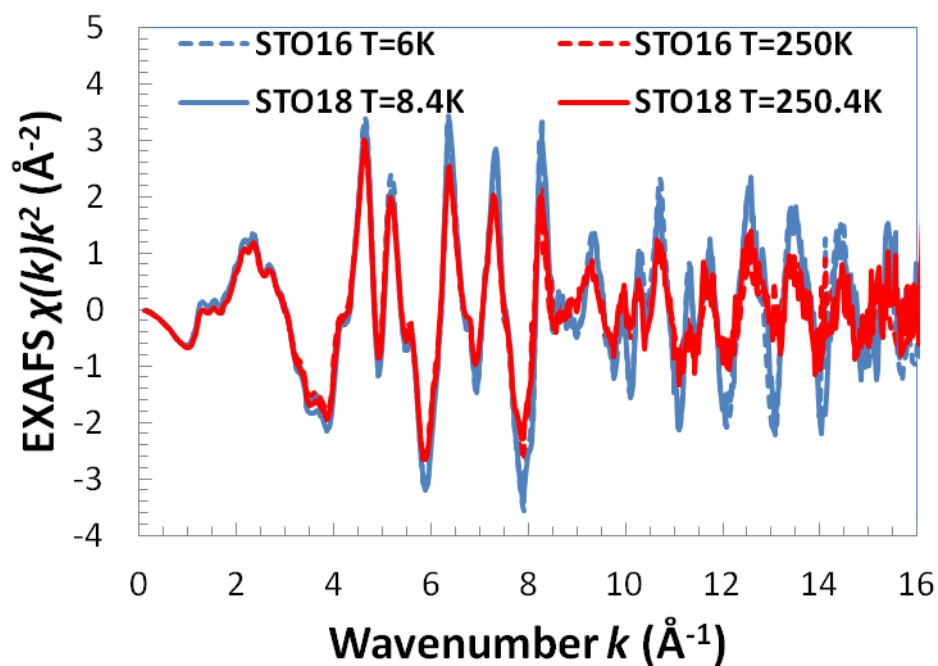


Fig.1. Ti K-edge EXAFS spectra for STO16 and STO18 at selected temperatures and their Fourier transform (FT). Note that the positions of the FT peaks are shifted from their true crystallographic values because the FTs were calculated without phase-shift corrections.

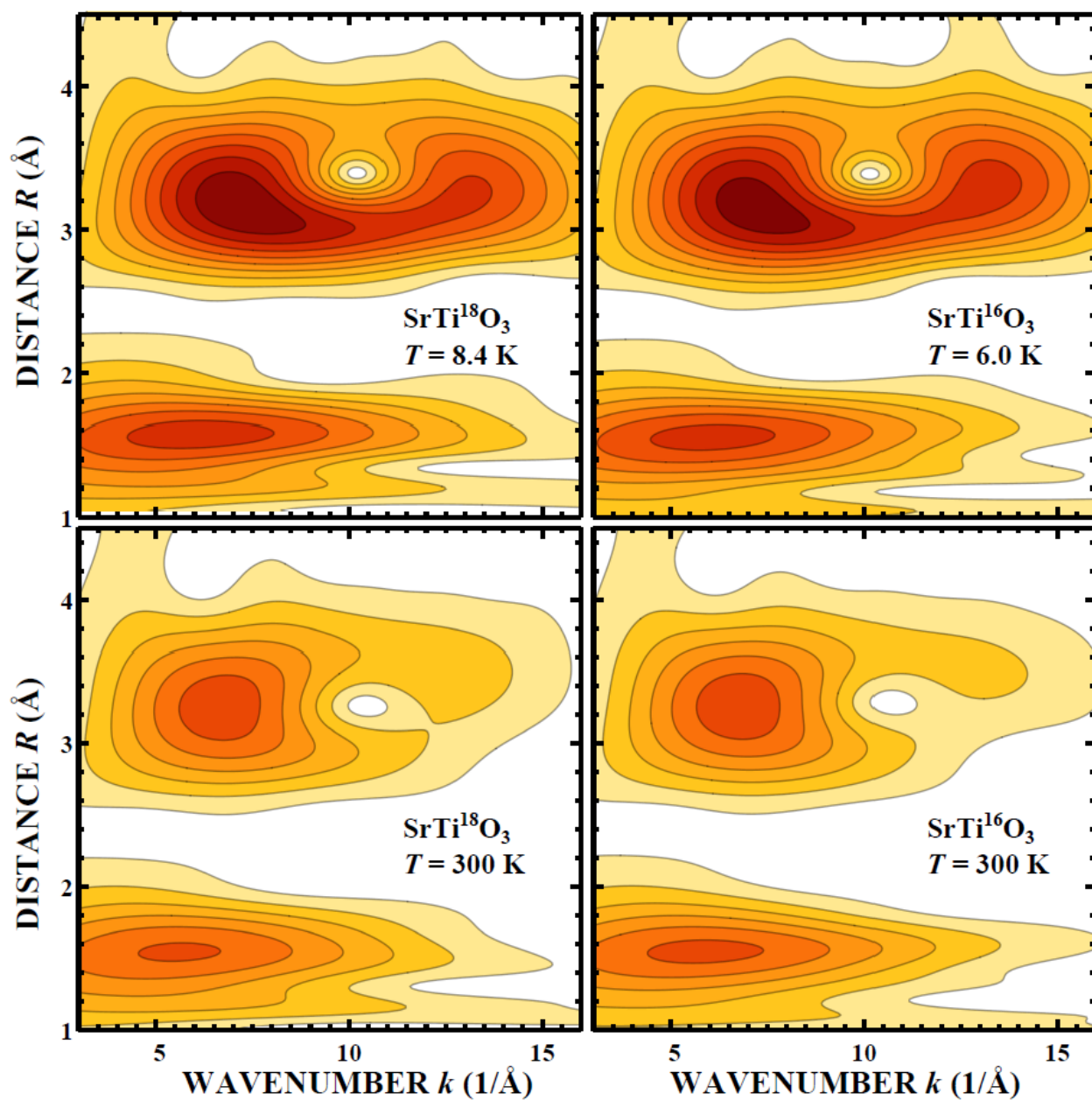


Fig.2. Wavelet analysis of Ti K-edge EXAFS data for STO16 and STO18 at selected temperatures, performed using Morlet wavelet transform.

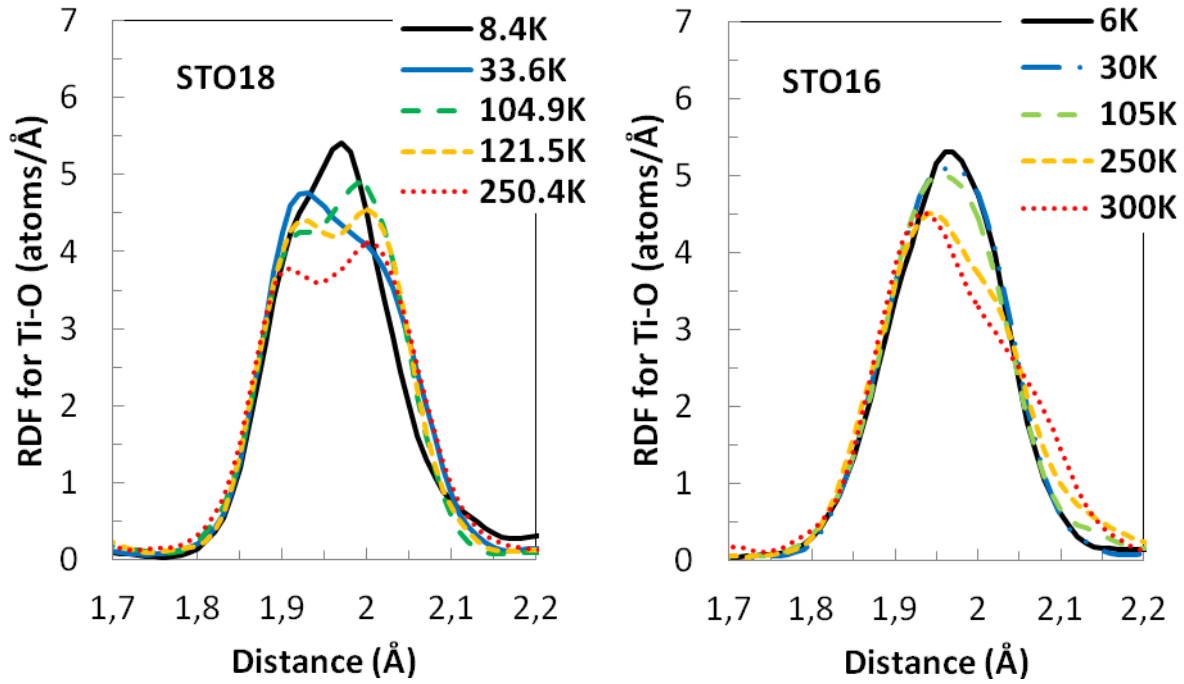


Fig.3. RDF for the first coordination shell of Ti (Ti-O).

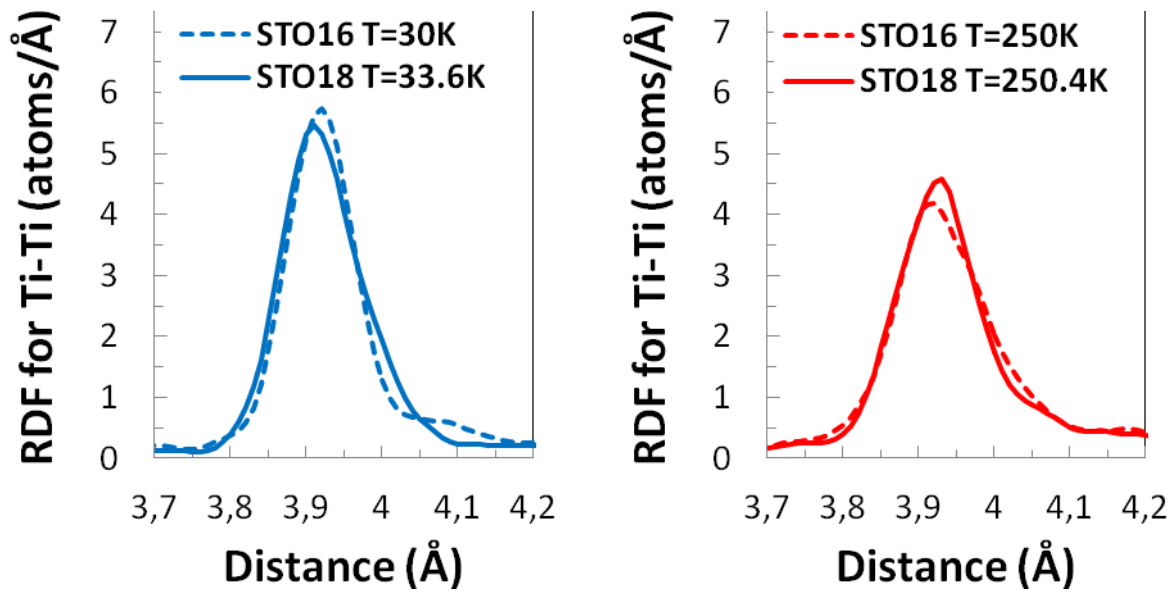


Fig.4. RDF for the third coordination shell of Ti (Ti-Ti).

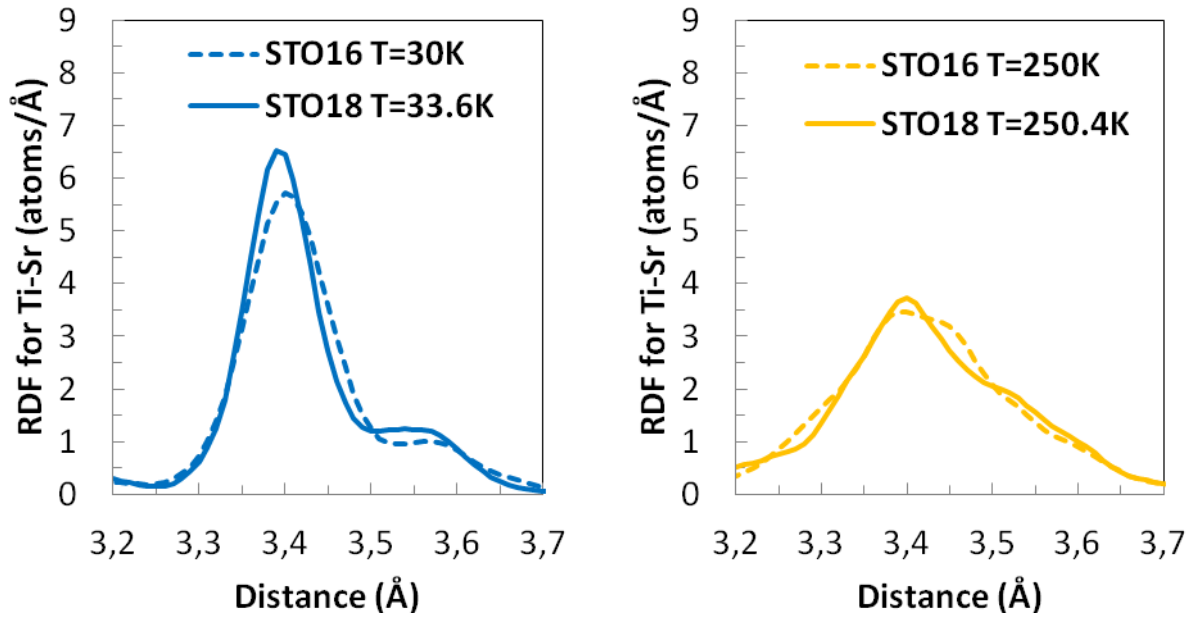


Fig.5. RDF for the second coordination shell of Ti (Ti-Sr).

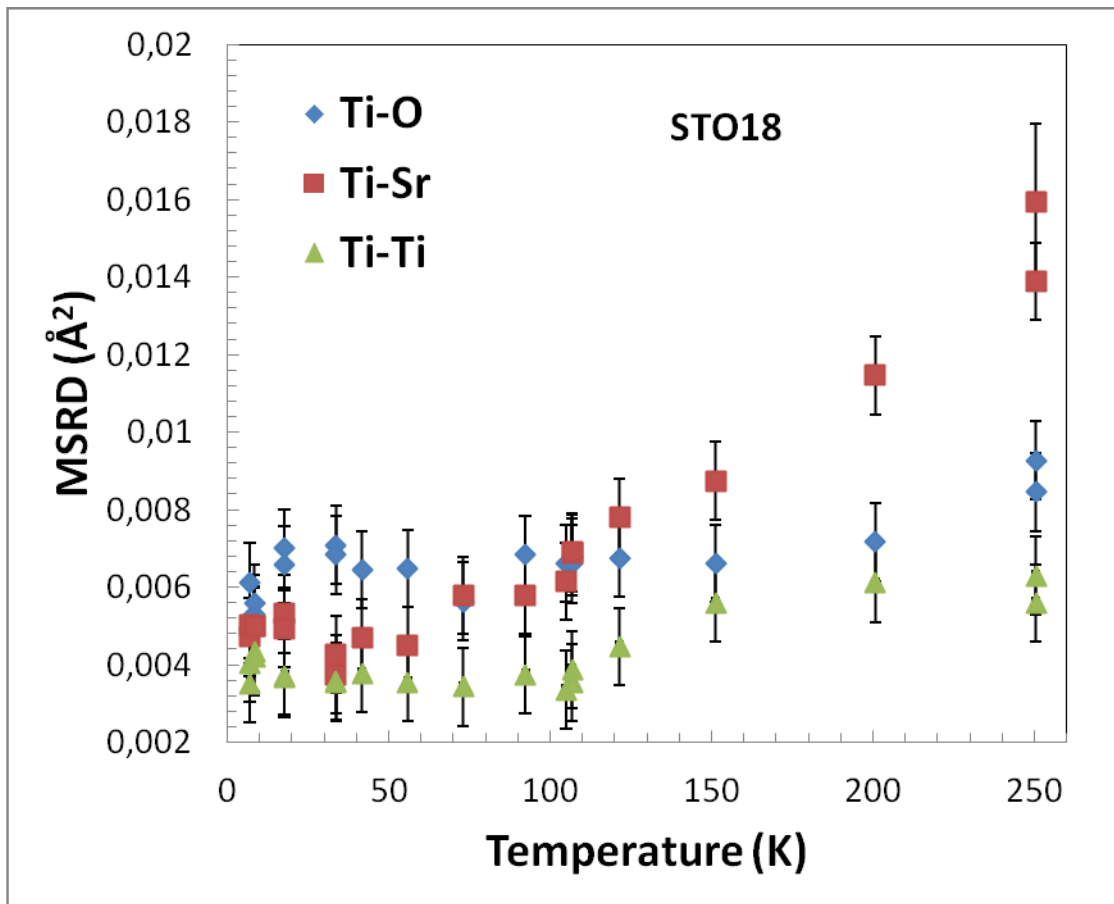


Fig.6. MSRD values for first three coordination shells of Ti.

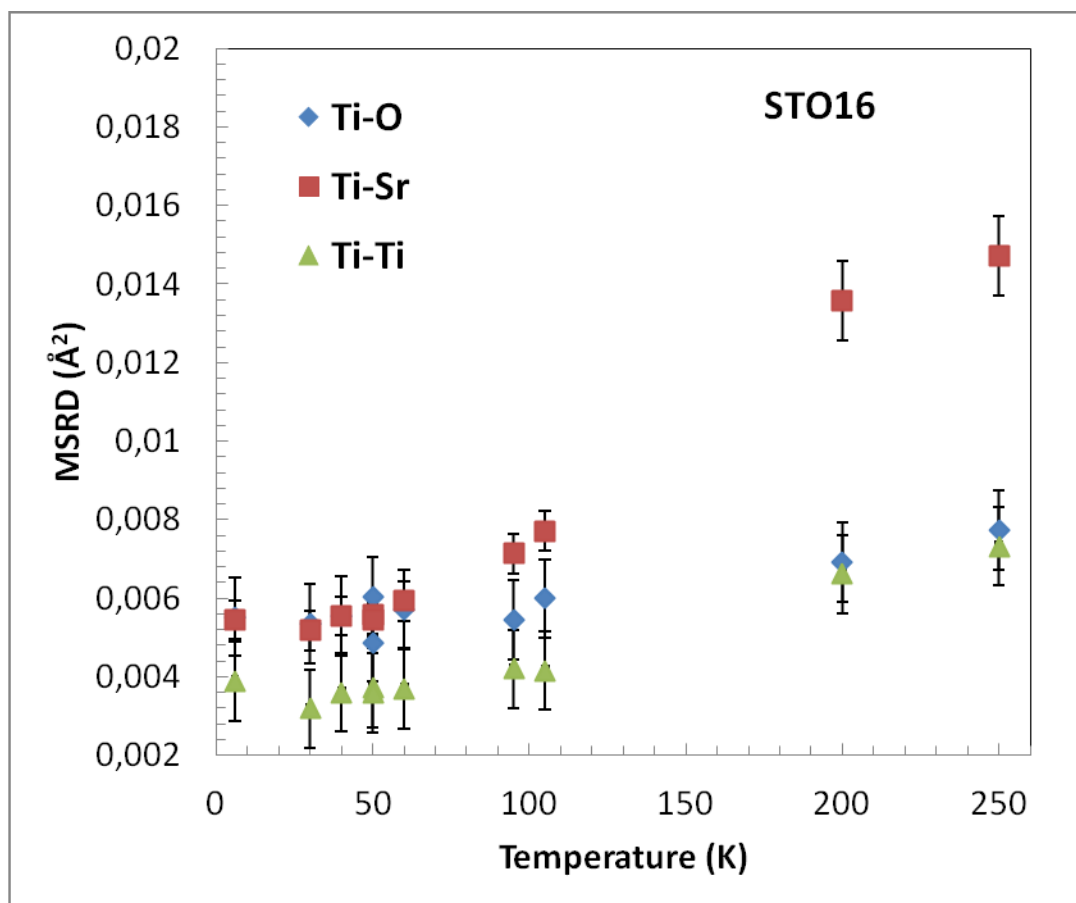


Fig.7. MSRD values for first three coordination shells of Ti.